Chem Soc Rev

Rational materials design for ultrafast rechargeable lithium-ion batteries

Journal:	*Chemical Society Reviews*
Manuscript ID:	CS-TRV-12-2014-000442.R1
Article Type:	Tutorial Review
Date Submitted by the Author:	05-Mar-2015
Complete List of Authors:	Tang, Yuxin; Nanyang Technological University, School of Materials Science and Engineering Zhang, Yanyan; Nanyang Technological University, School of Materials Science and Engineering; Nanyang Technological University, Li, Wenlong; Nanyang Technological University, School of Materials Science and Engineering Ma, Bing; Nanyang Technological University, School of Materials Science and Engineering Chen, Xiaodong; Nanyang Technological University, School of Materials Science & Engineering

Chem Soc Rev

TUTORIAL REVIEW

Cite this: DOI: 10.1039/x0xx00000x

Rational materials design for ultrafast rechargeable lithium-ion batteries

Yuxin Tang, Yanyan Zhang, Wenlong Li, Bing Ma, and Xiaodong Chen*

Received 00th October 2014,
Accepted 00th October 2014

DOI: 10.1039/x0xx00000x

www.rsc.org/

Rechargeable lithium-ion batteries (LIBs) are important electrochemical energy storage devices for consumer electronics and emerging electrical/hybrid vehicles. However, one of the formidable challenges is to develop ultrafast charging LIBs with the rate capability at least one order of magnitude (> 10 C) higher than that of the currently commercialized LIBs. This tutorial review presents the state-of-the-art developments of ultrafast charging LIBs by the rational design of materials. First of all, fundamental electrochemistry and related ionic/electronic conduction theories identify that the rate capability of LIBs is kinetically limited by sluggish solid-state diffusion process in electrode materials. Then, several aspects on the intrinsic materials, materials engineering and processing, and electrode materials architecture design towards maximizing both ionic and electronic conductivity in electrode with short diffusion length are deliberated. Finally, the future trends and perspectives for the ultrafast rechargeable LIBs are discussed. Continued rapid progress in this area is essential and urgent to endow LIBs with ultrafast charging capability to meet huge demands in the near future.

Key learning points

(1) Fundamental electrochemistry and ionic/electronic conduction theories.

(2) Key parameters to determine ultrafast charging.

(3) Intrinsic materials towards high-rate capability.

(4) Materials engineering and processing towards ultrafast charging LIBs.

(5) Electrode materials architecture engineering towards ultrafast charging LIBs.

1. Introduction

Lithium-ion batteries (LIBs), widely used to power the consumer devices (smart phones, laptops, tablets, etc.) and emerging electrical/hybrid vehicles, are reigning over current rechargeable battery markets attributing to their high energy density (> 180 Wh/kg, Figure 1) and great longevity (2-3 years). According to Frost & Sullivan research, global market of LIBs will reach around US$38 billion by 2020 due to the rapid growth of daily usages. As a result, the development of safe LIBs with large capacity, high energy and power density, as well as long lifespan is drawing much attention. Different advanced materials are mushrooming to substitute traditional electrode materials, offering great potential for next generation high power and energy LIBs. For instance, nanostructured silicon anode could deliver a high capacity around 4000 mAh/g, much higher than the traditional graphite anode (~ 372 mAh/g), which would reduce the electrode weight greatly. In addition, potential cathode candidates with high voltage, large capacity, as well as low environmental impact, are explored to replace $LiCoO_2$ (~ 140 mAh/g for practical application). Consequently, a series of new cathode compounds ($LiMn_xNi_yO_2$, $LiMn_xNi_yO_4$, etc.) are developed, and their specific capacity can reach up to 200 mAh/g according to the cut-off voltage, giving a higher energy density around 200 ~ 240 Wh/kg based on graphite electrode. Despite of the rapid progress on the capacity and energy density of LIBs, most of currently commercialized LIBs cannot replicate the convenience of filling up gasoline tank within several minutes, heavily limiting their application especially in battery electrical-powered vehicles (BEVs). The development of advanced LIBs with supercapacitor-like rate performance and battery-like capacity is an imperative direction that needs to be realized in the near future.[1]

The LIBs systems still suffer from sluggish charging because of low kinetics of Coulombic reactions involving electron transfer and ion diffusion in both anode and cathode materials.[1, 2] For the consumer electronics, the typical charging

School of Materials Science and Engineering, Nanyang Technological University, 50 Nanyang Avenue, 639798, Singapore.
Email: chenxd@ntu.edu.sg
http://www.ntu.edu.sg/home/chenxd/

time of LIBs ranges from 1 to 2 hours. For example, the iPhone 6 battery (ca. 1800 mAh capacity) generally takes long time (> 1.5 hour) to be fully charged with a standard 1 ampere (A) USB charger. Also, manufacturers recommend the charging time for 18650 cells (commonly used in laptops and cameras) should be longer than 1.2 hour. For the BEVs field, the U.S. Department of Energy (USDOE) launched Electrical Vehicles Everywhere Grand Challenge in 2012 to develop plug-in electric vehicles (PEV) by 2022, which requires both high power and energy density of LIBs (Figure 1). The development of PEV offers significant potential to reduce the dependence on the running-out gasoline and the emission of greenhouse gases. However, the fatal problem of current LIBs is that the energy density is decreased dramatically at high rates, far below the PEV goal. The trade-off between the power and energy density is expressed into Ragone plot in Figure 1. In view of these limitations, an ideal high-performance battery with charging rate (> 10 C) at least one order of magnitude higher than currently commercialized LIBs is highly desired to meet the future demands for BEVs as well as consumer electronics. The desired charging rate corresponds to a charging time less than 6 minutes, which is comparable to the fueling time of existing gasoline-powered cars.

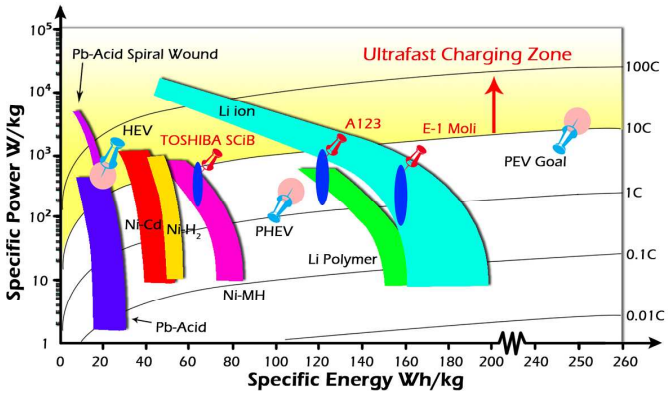

Figure 1. Specific energy and specific power of different battery types. The various PEV, plug-in hybrid vehicle (PHEV), hybrid electric vehicle (HEV) goals (blue drawing pins) were called by USDOE. The red drawing pins show some commercialized fast charging LIBs products. Curved lines indicate discharge rate.

In this tutorial review, we focus on the state-of-the-art material design strategies towards high-rate LIBs. First of all, basic electrochemistry fundamentals of LIBs and design guidance for achieving ultrafast rechargeable LIBs based on the understanding of conduction mechanism of Li-ion and electron transportation are provided. Secondly, we review the recent progress on intrinsic materials towards high-rate capability and rational materials design strategies to enhance diffusion kinetics of Li-ion and electron. Thirdly, apart from the materials aspect, the corresponding electrode architectures towards maximizing ion/electron transfer rate and transport pathways are also presented. Finally, based on the current development of ultrafast charging LIBs, the future challenges and opportunities in this direction are discussed. This review should shed light on the sustainable development of ultrafast charging LIBs by materials engineering and provide the basic guidance for designing high-rate LIBs performance.

2. Key Parameters to Determine Ultrafast Charging

2.1 Li-ion and Electron Diffusion Process in LIBs

LIBs utilize the reversible electrochemical reactions to convert and store electrochemical energy. To achieve high-rate LIBs performance, it is important to understand the Li-ion and electron transport pathways in the whole battery systems, and to increase the diffusion kinetics in the rate-limiting step. Taking discharging process as an example, Li-ion (blue dashed line) and electron (red dashed line) transportation can be identified in following steps (Figure 2).

① Li-ion and electron disassociate from the anode material simultaneously and move toward opposite directions via solid-state diffusion;
② Li-ion approach the electrode/electrolyte interface, and diffuse through the electrolyte;
③ The electron, driven by the higher potential of cathode side, pass through anode particles and their interfaces toward the current collector instead of riding into the electrolyte, and migrate via external circuit to power a device;
④ Electron and Li-ion enter the cathode materials concurrently via solid-state diffusion.

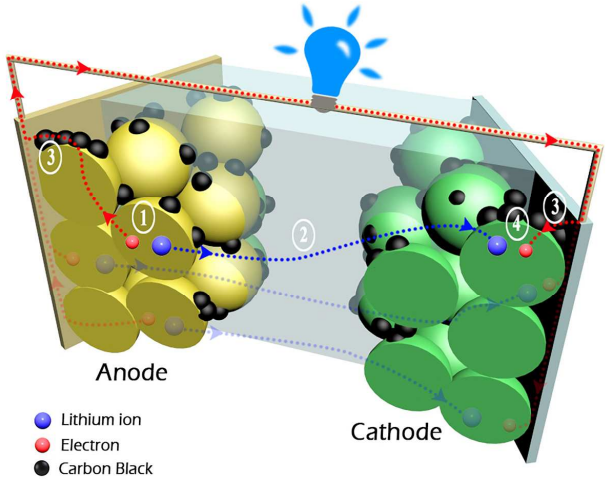

Figure 2. Transport pathways of Li-ion and electron in LIBs under discharging process.

2.2 Electrochemical Thermodynamics and Kinetics

From thermodynamic point of view, the energy release or storage in an electrochemical reaction is determined by reversible cell voltage (V) multiplying electron charges:

$$\Delta G_R = -nFV \quad (1)$$

where ΔG_R is Gibbs free energy change, n is number of electron transfer, F is Faraday constant. For battery systems, the energy density (E) is subject to the materials reversible capacity (Q) and operating voltage (V_{op}), which is generally determined by the Li-ion accommodation ability of active materials and electrochemical potential difference between their redox couples respectively.

$$E = QV_{op} \quad (2)$$

Power density (P), the rate of energy release/storage, is a kinetic characteristic to reflect current rate capability of LIBs. It can be expressed as:

$$P = \frac{QV_{op}}{t} = \frac{V_{op}^2}{R} \quad (3)$$

Where t is time; R is internal resistance. Normally the internal resistance is the sum of electronic resistance, ionic resistance and interfacial resistance (e.g., electrolyte and electrode, electrode and current collector or conductive additive). In describing charge current of batteries, it is often expressed as a C-rate in order to normalize against battery capacity. A 1 C rate means that the charge current will charge the battery to their theoretical capacity in 1 hour. With the C-rate increased to n C, the discharging/charging time is shortened to $1/n$ hour.

During an electrochemical reaction of LIBs (taking discharging process as an example), the difference between open circuit voltage (V_{oc}) and operating voltage (V_{op}) is termed as overpotential (η), which is the result of kinetic limitations. It is determined by:[3]

$$\eta = V_{oc} - V_{op} \quad (4)$$

The kinetic limitation[4] is mainly caused by: 1) activation polarization related to charge-transfer of electrochemical redox reaction; 2) ohmic polarization from the resistance of individual cell component and their interface; and 3) concentration polarization due to the mass transport limitation. The rate (current flow I) of a charge-transfer-controlled battery reaction can be given by the Butler-Volmer equation as:

$$I = I_0[\exp(\frac{nF\beta}{RT}\eta) - \exp(\frac{nF(1-\beta)}{RT}\eta)] \quad (5)$$

where I_0 $(=k_oFA)$ is the exchange current density; k_0 is reaction rate constant of electrode reaction; A is activity of the reactants, T is the Kelvin temperature; and β is transfer coefficient. From this, it is known that current density (reaction kinetic) is directly determined by the reaction rate constant, the activity of reactants, and the potential drop. The potential drop induced by activation polarization follows Tafel equation:

$$\eta = a - b\log I / I_o \quad (6)$$

which derived from Equation (5), where a and b are constants. Therefore, for high-rate application, the reactions with larger exchange current I_0 (higher k_0) and lower polarization are favored for improving electronic and ionic transport rate. This can be realized by rational materials and their electrode structure design, which can also significantly minimize ohmic and concentration/activation polarization by reducing the internal resistance and improving mass transport respectively. Since the rate performance depends on the transport kinetics of Li-ion and electron in electrodes and electrolytes, the fundamental understanding of their diffusion kinetics in solid-state and liquid phase steps (Figure 2) is of high importance.

2.3 Achieving high Li-ion Diffusivity in Electrode Materials

To figure out ionic conduction in solid-state diffusion of step (1) and (4) in Figure 2, we need to comprehensively understand the thermodynamic Li-ion diffusion mechanism. Ionic diffusivity (D_i), is a parameter to characterize the ease of Li-ion movement in the electrode materials. Typically, the dependence of diffusivity on temperature in solids is much higher than that in liquids, and the kinetics of diffusion process usually follows the Arrhenius relationship:

$$D_i = D_0 \exp\left(-\frac{\Delta G}{k_B T}\right) \quad (7)$$

Wherein ΔG is energy barrier; k_B is Boltzmann constant; and D_0 is the prefactor estimated empirically. For Li-ion diffusion in electrode materials, diffusion time (τ) can be expressed as:[5]

$$\tau = \frac{\lambda^2}{D_i} \quad (8)$$

Thus, to shorten the diffusion time, it is essential to enhance their diffusivity (D_i) in bulk or surface, or reducing their electron/ion diffusion length (λ) by using nano-size materials. From Equation (7), it is known that diffusivity is inversely exponentially proportional to energy barrier ΔG, thus a minor decrease of energy barrier can greatly increase the diffusivity. Although the increase of operating temperature (T) will enhance the diffusivity, it poses the potential safety problem for the battery working at high temperature.

2.4 Enhancing Li-ion Conductivity in Electrolytes

The main function of electrolyte is to bridge ionic connection between cathode and anode but to insulate electron. Therefore, electrolytes with high Li-ion conductivity (σ_{Li}) and low electronic conductivity are necessary for facilitating ionic transport and inhibiting the electron passage respectively. For LIBs application, it requires a high Li-ion conductivity of electrolyte (> 10^{-3} S/cm)[3] in the step (2) for rapid Li-ion motion at room temperature. In liquid phase, the relationship between ionic conductivity and diffusivity can be expressed as:[6]

$$\sigma_{Li} = \frac{q^2 c}{k_B T} D_L \quad (9)$$

Wherein D_L is diffusivity of the ion in the electrolyte, q is the charge of the ion, c is the concentration of the ion. D_L is theoretically given by Stokes-Einstein equation:

$$D_L = uk_B T = \frac{k_B T}{6\pi\mu R_0} \quad (10)$$

Wherein u is mobility of the ion, μ is the viscosity of the solution and R_0 is radius of the ion. It is found that the Li-ion diffusivity depends on the solvent composition through the electric field screening effect,[7] which means that the deintercalation/intercalation kinetics of Li-ion can be controlled by adjusting the solvent composition properly. To achieve higher conductivity σ_{Li} in the electrolyte, higher solubility of electrolyte and lower viscosity of electrolyte solution is preferred. Profited from these merits, organic liquid electrolytes (> 10^{-1} S/cm)[6] and gel electrolytes (currently used in commercialized LIBs, ~ 10^{-2} S/cm)[8] exhibit good Li-ion conductivity, which is high enough for the ultrafast ion transport since the σ_{Li} is several orders higher than that of conductivity in anode and cathode materials. While for the solid electrolytes (polymer electrolytes and inorganic solid electrolytes), their ionic conductivity is more than one order lower than that of liquid electrolytes. For examples, the polymer electrolyte possesses a conductivity ranging from 10^{-4} to 10^{-2} S/cm.[6] For most of inorganic solid electrolytes, their low ionic conductivity is smaller than 10^{-3} S/cm (perovskite $Li_{3x}La_{(2/3)-x}TiO_3$ with σ_{Li} of 10^{-5} S/cm, garnet $Li_7La_3Zr_2O_{12}$ with σ_{Li} of 5×10^{-4} S/cm, etc.).[9] Therefore, the increase of Li-ion solubility and the decrease of electrolyte viscosity are two important features to obtain high Li-ion conductivity.

2.5 Improving Electronic Conduction in Electrode Materials

Electronic conductivity (σ_e) of cathode and anode materials is also important in solid state diffusion process of step (4). Electrically conductive materials (like metallic materials and graphite) have very high electrical conductivity (> 1.0 S/cm), and their conduction is achieved by electron transport. For most of electrode materials, they have semiconductor features existing a gap between valence band and conduction band, and their conductivity is originated from their band structures. Taking both of electrons and holes into consideration, the electronic conductivity is given by:[10]

$$\sigma_e = n_i e \mu_e + p_i e \mu_h \quad (11)$$

Wherein n_i and p_i represent electron and hole concentration respectively; μ_e and μ_h represent mobility of electron and hole respectively.

For the intrinsic semiconducting electrode materials, only some electrons in valence band that near the Fermi level excited into conduction band due to thermal excitation. For every single excited electron, it leaves behind a hole in valence band. Thus, n_i is equal to p_i in the intrinsic electrode materials, the conductivity is given by:[10]

$$\sigma_e = 4.84 \times 10^{15} (\frac{m^*}{m_0}) T^{3/2} 3(\mu_e + \mu_h) \exp[-(\frac{E_g}{2k_B T})] \quad (12)$$

in which m^*/m_0 is the effective mass ratio for electron and hole (by assuming $m_e^* = m_h^*$); E_g is bandgap of the electrode materials. For the extrinsic semiconductor, the doping of electrode materials introduces different concentrations of holes and electrons. Thus, electronic conduction of semiconductors in Equation (11) is dominated by majority electrons or holes movement in n-type or p-type electrode materials respectively.

Therefore, to achieve high-rate LIBs, it is essential to select electrode materials with high intrinsic electronic conductivity (e.g., smaller bandgap or zero bandgap, Equation 12). Apart from that, external methods are also important, like conductive agent addition and doping technology. For example, electron can diffuse faster than Li-ion in electrode materials with conductive additives adding, and the doping can drastically increase the conductivity of materials by introducing extrinsic charge carriers (Equation 11). Furthermore, the ionic conduction of electrode materials also needs to be considered since the overall conduction consists of both electron and ion movement. For example, although zero band gap graphite possesses high electronic conductivity, its ionic conductivity is low (10^{-10} ~ 10^{-8} S/cm),[6] which limits its high-rate application.

To sum up this section, it is known that the high-rate performance in terms of energy and power density is related to thermodynamics and kinetics of electrochemical reaction, and the rate capability of the LIBs is kinetically limited by the slow solid-state charge diffusion and transfer processes in the electrode materials. Therefore, the choices of materials candidates and rational materials design to enhance diffusion kinetics of Li-ion and electron in electrode materials are important to achieve high-rate LIBs.

3. Intrinsic Materials towards High-rate Capability

According to discussion on thermodynamics and kinetics of electrochemical reaction and diffusion steps in Section 2, the high-rate performance LIBs require both the anode and cathode materials possess high-rate capability simultaneously with high reversible capacity. Therefore, electrode materials need to meet the following requirements: 1) fast electrochemical reaction kinetics with Li-ion and electron; 2) high ionic diffusivity and electronic conductivity; 3) short diffusion length for electron and ion; and 4) robust structure for rapid insert/removal of Li-ion. In the past decade, science venture on high-rate electrode materials has been widely explored, and some of them have rapidly evolved into viable choices in LIBs industry. Significant developments of electrode materials for high-rate LIBs are summarized in Figure 3 and discussed as follows.

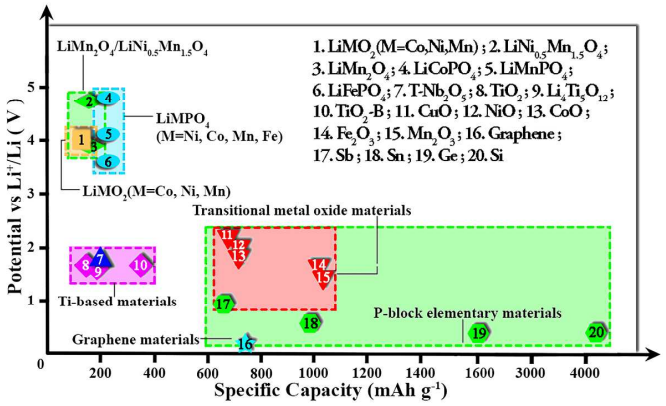

Figure 3. Voltage versus capacity chart for anode and cathode materials for high-rate LIBs application.

3.1 High-rate Anode Candidates

The development of suitable high-rate anode candidates with high capacity, ease diffusion of Li-ion, along with good cycling life and free from safety concerns is highly desirable to replace graphite anodes. The diverse alternatives have been sprung up, and the reaction mechanisms between lithium ion and electrode materials can be distinguished as intercalation-, conversion-, and alloy- reactions, as shown in Figure 4.

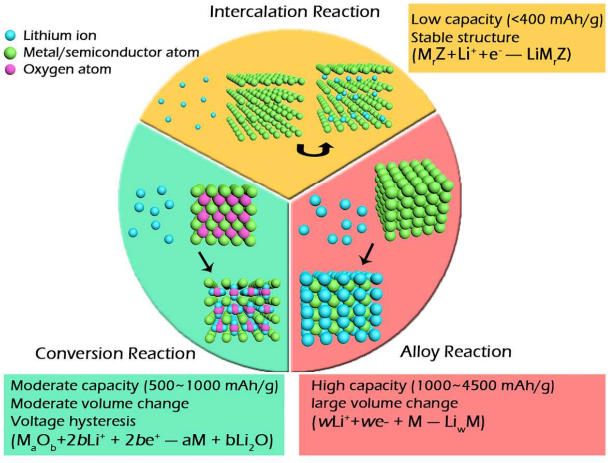

Figure 4. A schematic representation of three typical reaction mechanisms between lithium ion and electrode materials.

Intercalation Materials: Insertion compounds include carbon allotropes (graphene and carbon nanotube), TiO_2-based materials, orthorhombic Nb_2O_5 (T-Nb_2O_5), etc. These materials are capable of providing fast Li-ion reaction kinetic (possessing Li-ion conductive 1D paths or 2D planes) and maintaining structural integrity upon cycling due to robust open framework with low volume expansion, which are desirable for high-rate and long-lasting LIBs. However, most of insertion materials have relatively low theoretical capacities (limited to one electron storage per *M* ion, Figure 3) due to finite

accommodation sites. Carbon allotropes, such as graphene, or graphene oxide and carbon nanotubes (CNTs), show attractive features for high-rate applications in terms of better electronic conductivity, larger surface area, shorter diffusion length and higher Li-ion storage capacity (around 2 times) than that of graphite.[11] However, like graphite, graphene and CNTs also face intrinsic safety issues due to the low lithiated potential.[11] On the other hand, the exploration of them as conductive additive or electrode support for high-rate LIBs is promising because of their excellent conductivity, chemical stability, and mechanical robustness.

Another class of candidates is titanium oxide-based materials (TiO_2, $Li_4Ti_5O_{12}$, etc.) with merits of safe lithiation potential (> 1.5 V versus Li^+/Li), low volume change (< 5%), and excellent reversible capacity. They have drawn great attentions for fast rechargeable LIBs even though they own low intrinsic ion and electron conductivity.[12] Currently, $Li_4Ti_5O_{12}$ has been commercially used for ultrafast charging battery and shown superior cycling stability and calendar life more than thousand cycles. A recent work on carbon-coated $Li_4Ti_5O_{12}$ nanoporous microsphere showed remarkable improvement in rate capability of 126 mAh/g at 20 C.[12] For TiO_2 allotropes, TiO_2-B with layered structures, possessing favorable open channels for lithium ion mobile and highest theoretical specific capacity (335 mAh/g) among the TiO_2 polymorphs, holds a distinct advantage of pseudocapacitive charging mechanism for ultrafast charging.[13] Our recent work demonstrated an elongated TiO_2(B) nanotubular cross-linked network anode material could cycle over 10000 times while retaining a relatively high capacity (114 mAh/g) at an ultrahigh rate of 25 C (8.4 A/g).[14] Based on the same intercalation pseudocapacitance mechanism, T-Nb_2O_5 materials offering 2D transport pathways and little structural change upon insertion, is also a promising candidate as high-rate anode.[15]

Alloy Materials: Alloy compounds Li_xM (M = Si, Sn, Ge, etc.) deliver the highest volumetric and gravimetric energy density (Figure 4) since they can store multiple Li-ion (per *M*). Thus, the material candidates are applicable for ultrahigh-power LIBs applications. As shown in Figure 3, silicon possesses the highest theoretical capacity of 4200 mAh/g (corresponding to $Li_{4.4}Si$ form). Likewise, Ge has a theoretical capacity of 1600 mAh/g ($Li_{4.4}Ge$), and Sn has a smaller specific theoretical capacity of 960 mAh/g ($Li_{4.2}Sn$) owing to its larger atomic mass. However, their significant drawbacks, such as low Li-ion reaction kinetic and severe volume change upon lithium insertion-extraction (leading to pulverization and amorphization of electrode particles), severely compromise rate-capability and cycle life of LIBs.[16] Therefore, materials engineering to enhance their high-rate performance and stability is essential. For example, a robust double-walled silicon nanotube (DWSiNT) anode,[17] consisting of a confined SiO_x layer forming a stable solid electrolyte interfaces (SEI) and an inner Si layer accommodating Li-ion insertion, maintained a high capacity of 540 mAh/g at a rate of 20 C, and retained 88% of its initial capacity at 10 C after 6000 cycles.

Conversion Materials: Conversion compounds M_aO_b (M = Co, Fe, Ni, Mn, Cu, etc.), discovered by Tarascon, J. M. et al,[18] have been extensively studied due to their high specific capacity via the multiple electron reaction per *M* (Figure 3). During the electrochemical reaction, these oxides are converted to a metallic state along with Li_2O component at the first lithiation and are reversibly returned to its initial state after delithiation. For the conversion systems, the reaction potential is normally within 0.5 ~ 1.0 V, and it increases with the ionicity of M−O bond.[11] The safer lithiated potential and higher specific capacity of conversion materials are important characteristics for high-rate LIBs. However, poor reaction kinetics, large volume expansion and large potential hysteresis, related to the energy barrier in the breaking of the M−O bond and the change of electronic conductivity, still limit them for high-rate applications in terms of electrochemical performance and long-time stability.[2,11] In this regards, the nanostructured porous materials and their nanocomposites with high reaction kinetic have been developed to improve the capacity retention and the stability of SEI film at high rates. For example, a multishelled Co_3O_4 hollow microspheres[19] exhibited a high specific capacity of 1117 mAh/g at a current density of 2 A/g while the commercial Co_3O_4 can only delivered a capacity of 206 mAh/g.

3.2 High-rate Cathode Candidates

The lithiation/de-lithiation process for most of cathode materials is based on the insertion mechanism, wherein Li-ion are inserted and removed from planes or tunnels in the host structure. The well-known high-rate cathode materials (Figure 5) include layered oxides ($LiCoO_2$, $LiMnO_2$, $LiNi_{0.5}Mn_{0.5}O_2$, $LiNi_{1/3}Co_{1/3}Mn_{1/3}O_2$), spinel oxides ($LiMn_2O_4$, $LiNi_{0.5}Mn_{1.5}O_4$), olivine polyanions $LiMPO_4$ (M = Fe, Co, Ni, Mn), etc. These cathode materials have a limited capacity due to the limited seating sites for lithium ion (up to one lithium ion per *M*), and their rate capability mostly depends on their electronic and ionic conductivity, which is related to the dimensionality of Li-ion transport within their crystal structures.[20, 21]

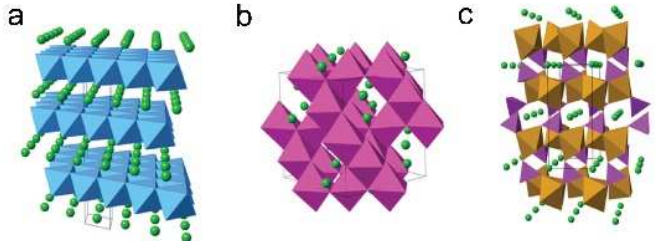

Figure 5. Representative crystal structures of high-rate LIBs cathode materials: (a) layered $LiCoO_2$, (b) spinel $LiMn_2O_4$; and (c) olivine structured $LiFePO_4$.[20] Reproduced from Ref. 20 with permission from Royal Society of Chemistry.

Layered oxides: $LiCoO_2$, providing fast 2D Li-ion diffusion channels through the CoO_2 interlayers constructed by the CoO_6 octahedral via sharing edges (Figure 5a), is suitable for high-rate cathode. However, $LiCoO_2$ remains some challenging issues like structural instability, resulting from weak van der waal's interaction between CoO_2 layers. Thus, it can only deliver about 140 mAh/g capacity (half of the theoretical capacity). Besides that, high cost and environmental issue due to the use of the expensive and toxic Co are also the limiting factors. In view of this point, the replacement of Co ion into environmental friendly Ni and Mn ion ($LiNi_{0.5}Mn_{0.5}O_2$ and $LiNi_{1/3}Co_{1/3}Mn_{1/3}O_2$) could improve the materials stability and maintain the rate capability simultaneously.[11] Recently, an disordered cathode material ($Li_{1.211}Mo_{0.467}Cr_{0.3}O_2$) with excess lithium, transformed from the well-ordered layered pristine materials after few charging-discharging cycles, could provide efficient channels for Li-ion percolation with high capacity (265.6 mAh/g). This type of disordered-electrode materials is very promising for high-rate LIBs application.[22]

Spinel oxides: Spinel $LiMn_2O_4$ is an attractive cathode material for high-rate applications due to its unique 3D pathways for fast Li-ion transport in all directions (Figure 5b). However, $LiMn_2O_4$ has problems related to severe capacity fading upon prolonged cycling mainly due to the dissolution of Mn^{2+} into the electrolyte and generation of new phases.[21] Similarly, the $LiNi_{0.5}Mn_{1.5}O_4$ also exhibited the poor cyclability due to the chemical instability. Although the crystal structure of spinel materials favor high-rate application, their intrinsic Li-ion diffusivity and electronic conductivity is more than one order of magnitude less than that of $LiCoO_2$, limiting the high-rate performance.[6] Thus, the electrode structuring, doping method and surface coating are important to enable the rapid charge transport kinetic and low resistance pathways required for high-rate LIBs. For examples, carbon coating on $LiMn_2O_4$ was applied to prevent the dissolution of Mn^{2+} and enhance rate performance,[23] and Ru-doped $LiNi_{0.5}Mn_{1.5}O_4$ showed a high capacity of 135 mAh/g at 10 C, with a 82.6% capacity retention after 500th cycle using 10 C charging and discharging rates.[24]

Olivine polyanions: Olivine $LiFePO_4$ (Figure 5c), enjoying the merits of safety, high thermal stability, environmental compatibility and low cost, is widely studied for high-rate cathode materials. Compared with layered and spinel materials, its structural stability is enabled by the strong bonding of O-P (in PO_4^{3-} polyanions) and O-Fe, ensuring the long-time cyclability. However, the poor rate capability is limited by the 1D Li-ion transport channels and low Li-ion diffusivity and electron conductivity resulting from the insulating PO_4^{3-} polyanions framework.[20] To address the rate limitation of these materials, several approaches have been proposed to improve the conductivity, such as size tailoring, surface modifications, doping, and so on.

To end this section, it is worth noting that the high-rate LIBs require both the anode and cathode materials simultaneously possess high-rate capability, thus the intrinsic property of high ion and electron conductivity is an important feature. However, since most of the electrode materials have the semiconductor features, their conductivity is not so ideal to meet the requirements. For examples, the Li-ion diffusivity of $LiCoO_2$, $LiMn_2O_4$, and $LiFeO_4$, ranges from 10^{-15} to 10^{-8} cm^2/s and their electronic conductivity ranges from 10^{-9} to 10^{-4} S/cm.[6] Based on Equation (8), to achieve ultrafast Li-ion insertion through the active materials within 6 min, its characteristic size should be less than 190 nm with a ionic diffusivity of 10^{-12} cm^2/s. Therefore, proper materials engineering and electrode structure design towards short diffusion length and high ionic/electronic conductivity are important to achieve high-rate LIBs performance and the detailed discussions are provided in the next section.

4. Materials Engineering and Processing towards High-rate LIBs

The solid-state charge diffusion is the kinetically limited step during electrochemical reaction (Figure 2). From the materials perspective, the rational design of electrode materials with high electron/ion diffusion constants in their bulk or surface, or reducing their electron/ion diffusion length by using nano-size materials is required according to the ion/electron conduction mechanism. To this end, beyond nanostructuring strategy, dopant manipulation, surface modification (or coating), Li-ion diffusion control, and hybrid-composite design can increase the ionic and electronic conductivity of the electrode materials in the bulk and the surface respectively. For example, the surface coating can facilitate the electron or ion transport across the electrode/electrolyte interface and form a stable SEI layer to alleviate side reactions. These approaches are summarized in Figure 6.

4.1 Nanostructuring Strategy

In order to have short solid-state diffusion length (λ) and high surface area to enhance transportation rate of ion and electron within active material (Equation 8), nanostructuring strategy has been adopted to fabricate 0D nanoparticles, 1D nanotubes/wires, 2D sheets or films, and 3D porous or hollow structures of the active materials. For high surface area of nanoscale materials, the rate performance is enhanced by the increase of interfacial electrochemical reactions and the higher flux of Li-ion across the electrode–electrolyte interface, thus the increasing of charge transport efficiency as well as the reducing of thermodynamic energy barrier can be realized.[19, 23] For example, a hierarchical and mesoporous structure of LTO spinel frameworks[23] with a high surface area of 205 m^2/g (Figure 7a) demonstrated the combined properties of both batteries (high energy density) and supercapacitors (high power densities) up to high rate of 400 C (Figure 7b). Beyond the consideration of achieving high surface area, the intrinsic property of materials is also important. For example, we recently discovered that the nanotubular aspect ratio is a critical parameter to determine the electrochemical performance.[25] It is found that the battery performance at high rates is dramatically boosted when the aspect ratio is increased, due to the optimization of electronic/ionic transport properties within the electrode materials (Figure 7c-d).[25] The fundamental understanding should be useful in the development of efficient LIBs devices by exploiting the properties of unique nanostructures.

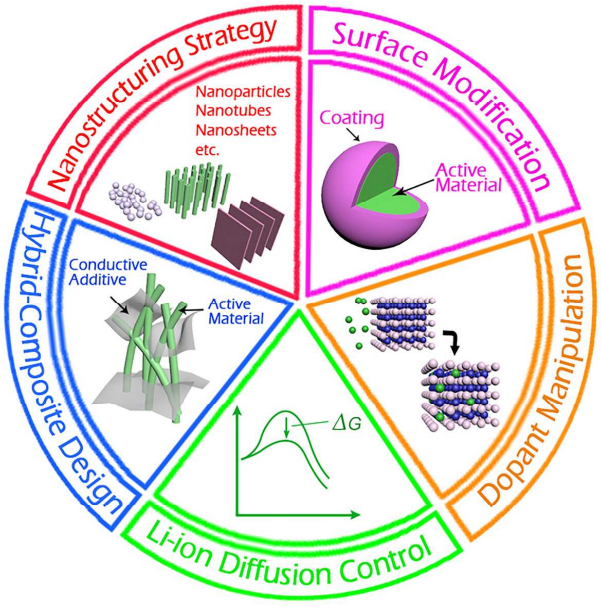

Figure 6. Materials engineering strategies towards high-rate LIBs.

4.2 Surface Modification

The surface chemistry modification is an appealing approach to enhance the electronic- and/or ionic- conductivity (Equation 8) as well as to stabilize the SEI layers. There are two main kinds of adopted conducting materials, namely carbon/metal materials, and metal oxides-based materials. The carbon coating is a common

technique used to enhance the surface electronic conductivity of electrode materials. Cho et al. reported an electrical network composed of thin carbon layer coated on spinel $LiMn_2O_4$ nanoclusters (Figure 8a) for ultrahigh rate LIBs.[26] This approach increases rate capability and maintains excellent electrode energy density concurrently. It retains a high value (ca. 47%) of the initial capacity even at 300 C (Figure 8b). Another kind of conductive coating is metallic materials. For example, Au-cobalt oxide nanowires, assembled first via a virus-mediated process and then incorporated with gold nanoparticles, showed the improved performance at high rate compared with that of the pure Co_3O_4 nanowires.[27] Besides the conventional carbon or metal coatings, other substances with high electronic conductivity were also explored. Park K. et al.[28] reported that a surface conductive TiN layer would enhance the electronic conductivity of LTO materials greatly, generating 6 times larger capacities (ca. 120 mAh/g) than that of the pristine LTO at 10 C.

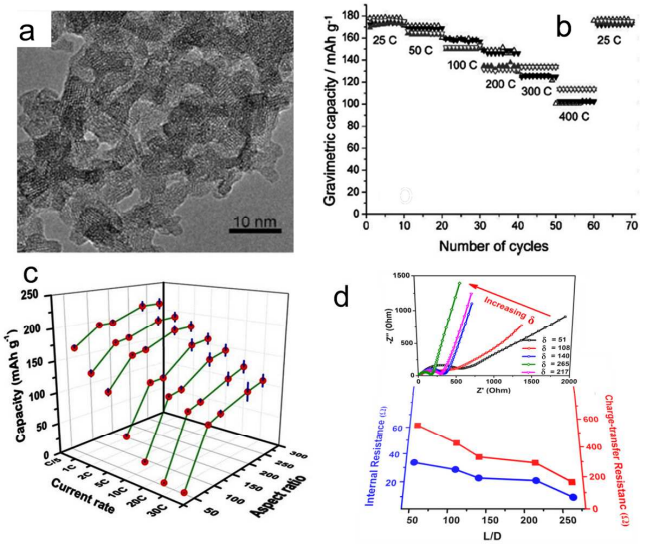

Figure 7. Nanostructuring strategy: (a) TEM images and (b) high-rate performance of porous framework of lithium titanate.[23] (c) The correlation between the aspect ratio and the capacity of different TiO_2 nanotubes at various discharging rates; (d) Nyquist plots of the nanotubes electrodes (top) and the correlation (bottom) between the aspect ratio and internal resistance and charge-transfer resistance of various nanotube electrodes.[25] Reproduced from Ref. 23 and 25 with permission from John Wiley & Sons Ltd.

Contrary to the conventional usage of electronic coatings, attempts have been made to coat low ionic conductivity materials with high ones to improve their Li-ion diffusion kinetics. For instance, the rutile-TiO_2 coating on LTO nanosheets showed much improved rate capacity (around 120 mAh/g), about 6 times higher than that of pure LTO nanosheets at 60 C due to the significant enhancement of surface ionic conductivity from TiO_2 phase.[29] Apart from the anodes, a surface chemistry modification on $LiFePO_4$ cathode materials (Figure 8c) through controlled off-stoichiometry ($LiFe_{0.9}P_{0.95}O_{4-\delta}$) provided an ultrafast ion transport rate at the surface, achieving an extremely high-rate capacity of more than 100 mAh/g at 197 C (Figure 8d).[30] Interestingly, a smart approach based on the full-concentration gradient (FCG) nickel lithium transition-metal oxide had led to success in harnessing the high power/energy density as well as achieving longevity.[31] When discharged at 5 C, the FCG material delivered the highest reversible capacity among the controlled cathode materials due to the high diffusion coefficient of lithium ion originated from the outside coating of the percolated nanorods network. In addition, the manganese-rich outer layers can also stabilize the material and provides high thermal stability, especially during high-voltage cycling. These works made it clear that the surface chemistry plays an important role in improving rate performance as well as cycling life in terms of electronic/ionic-conducting media, which facilitates the charge transfer at the particle surface. In addition, the coating layer can act as a physical protection barrier that impedes the side reactions between electrode materials and electrolytes, elongating the lifetime of LIBs.

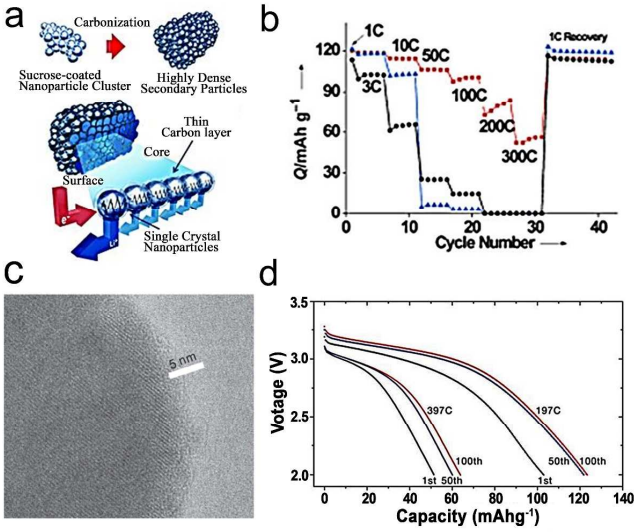

Figure 8. Surface modification to enhance the ionic and electronic conductivity: (a) Configuration of carbon-coated single crystal $LiMn_2O_4$ (CSC); (b) Rate capabilities for CSC (red square), single-crystal $LiMn_2O_4$ nanoparticles (blue triangle), and polycrystalline $LiMn_2O_4$ microparticles (black dot).[26] (c) TEM image for $LiFe_{0.9}P_{0.95}O_{4-\delta}$ nanoparticles with a conducting layer; (d) Discharge capability at very high rate for $LiFe_{0.9}P_{0.95}O_{4-\delta}$.[30] Reproduced from Ref. 26 with permission from John Wiley & Sons Ltd. Reproduced from Ref. 30 with permission from Nature Publishing Group.

4.3 Dopant Manipulation

The doping method is to introduce homogenous/heterogeneous metal (nonmetal) ion or vacancy into the materials bulk matrix to enhance its conductivity due to deficiency or excess of electron (Equation 11), improving the battery performance. For example, by substitution of carbon atoms on edges or defect sites with N or B (Figure 9a), N- or B- doped graphene anodes[32] deliver high power and energy densities (Figure 9b) due to the enhancement of Li-ion intercalation and conversion reaction rate as well as electrical conductivity. A high capacity of 199 mAh/g and 235 mAh/g was obtained from the N-doped and B-doped graphene at 25 A/g (about 30 s to fully charging) respectively. With the similar concept, the intrinsic doping of Ti^{3+} in LTO nanowires was fabricated through hydrogenation process.[33] As a result, the rate capacity of hydrogenated $Li_4Ti_5O_{12}$ (H-LTO) nanowires are three times greater than that of the pristine LTO nanowires, delivering a high capacity of 121 mAh/g at 30 C. Impressively, black anatase TiO_2[34] induced by the similar hydrogenation process (Figure 9c) delivered a high capacity of 152 mAh/g at ultrahigh rate of 100 C (Figure 9d).

4.4 Li-ion Diffusion Control

To enhance Li-ion conduction in solid-state diffusion process, beyond the nanostructuring strategy to minimize the diffusion length, it is also important to increase the lithium-ion diffusivity via

the reduction of activation energy (Equation 7). For example, a strategy to increase Li-ion diffusivity by reducing the activation energy via minimizing the strain effect as well as the electrostatic interaction (between the Li^+ and the transition-metal cation) was reported on $Li(Ni_{0.5}Mn_{0.5})O_2$ cathode materials.[35] According to the computational calculation, the large space between the oxygen layers with less Li-Ni sites disordering can reduce the activation energy greatly (Figure 10a). This calculation leads to a novel ion-exchange experiment, which enables the synthesis of $Li(Ni_{0.5}Mn_{0.5})O_2$ with less interlayer disordering of Li-Ni sites. Thus, this cathode material delivered higher capacity at ultrahigh rate compared with the traditional method (Figure 10b).

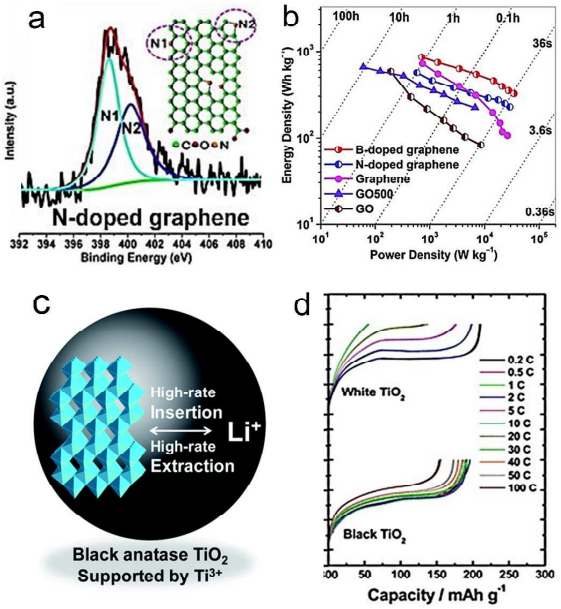

Figure 9. Dopant manipulation for high-rate LIBs: (a) XPS spectrum and (b) Ragone plots for the pristine graphene, N-doped graphene, B-doped graphene and graphene oxide (GO) electrodes.[32] (c) Schematic drawing of the mixed valency in anatase TiO_2 and (d) rate capability for the white and black anatase TiO_2.[34] Reproduced from Ref. 32 with permission from American Chemical Society. Reproduced from Ref. 34 with permission from Royal Society of Chemistry.

Engineering the crystallographic orientation to match the ionic diffusion pathways is another route to decrease the lithium ion diffusion energy barrier. An original contribution clarified the passionate debates about how the electrochemical extraction of Li^+ occurs in $LiFePO_4$ via a "domino-cascade" mode confirmed by experimental observations.[36] This study revealed that the process of lithiation/delithiation within $LiFePO_4$ is directionally dependent, with diffusion being mainly confined to channels along the b axis. From this point of view, the facet control of the $LiFePO_4$ is required towards the high-rate application. For examples, $LiFePO_4$ nanoplates with the {010} facet prominent delivered a capacity five times larger than that of nanoplates with the {100} facet prominent at 10 C.[37] In addition, a liquid-phase exfoliation method was reported for the fabrication of $LiMPO_4$ (Fe, Co, Mn) ultrathin nanosheets with exposed (010) surface facets.[38] The excellent rate capabilities are achieved since the diffusion time for Li^+ to diffuse over a [010]-thickness is about 5 orders of magnitude lower than the corresponding bulk materials. Besides that, engineering the crystallographic orientation with graphene layers was also explored.[39] The oriented graphene layers perpendicular to the surface substantially maintained a higher capacity (35% of initial capacity at 0.05 C) at 10 C while the graphene layers paralleling to the film surface shows little capacity (0% of initial capacity), which is due to easy release of stress in orientated graphene samples during Li^+ insertion. These superior high-rate capabilities exemplify how crystal orientation tuning critically affects the high-rate performance of electrode materials.

4.5 Hybrid-composite Design

A hybrid-composite approach is also an effective solution in enhancing the electronic and ionic transport rate of electrode materials. The approach is to synthesize composited materials with by incorporating the conducting additives (such as carbon-based materials, conducting polymers, or metallic compounds) into the electrode materials, which is different from the coating technology. The conducting materials act as electron pathways that electrically interconnect the electrode materials, ultimately providing the electrode with a high conductivity. Also, the adding of conducting materials reduces lithium ion diffusion length of the particles, providing the electrode materials with fast kinetics for the lithium ion insertion and de-insertion. For instance, a hierarchical Si-C composite materials[40] (Figure 11a), showed an outstanding capacity of 1590 and 870 mAh/g at 1 C and 8 C respectively while the annealed carbon black only delivered limited capacity (40 mAh/g at 8 C). This is because that the irregular channels inside the Si-C composite enable rapid access of Li-ion into the bulk particle and large Si volume change is accommodated by the internal porosity of particles. Furthermore, a well-organized carbon nanotube (CNT)@TiO_2 core/porous-sheath coaxial nanocable (Figure 11b),[41] in which CNT core provides sufficient electron for the storage of Li-ion in TiO_2 sheath and nanoporous TiO_2 favors the penetration of Li-ion to the CNT core, showed minor capacity decrease when current density increases even to 5 A/g. Beyond that, interesting works of hybrid-composited materials on sandwiched structure of graphene-MnO_2-graphene[42] and LTO-carbon aggregated particles[43] also showed outstanding LIBs performance at high rates. For example, the LTO-carbon composites (Figure 11c) can be effectively cycled at current rates as high as 20 C while still maintaining a capacity delivery of 156 mAh/g, which is 89% of the maximum theoretical value (Figure 11d). Besides the inorganic composited materials, a recent work on organic/graphene cathode composite was also explored. The poly (2,2,6,6-tetramethylpiperidinyloxy-4-yl methacrylate) (PTMA)/graphene[44] could deliver 80 mAh/g even at a high rate of 200 C, suggesting the outstanding rate capability of the PTMA/graphene composite.

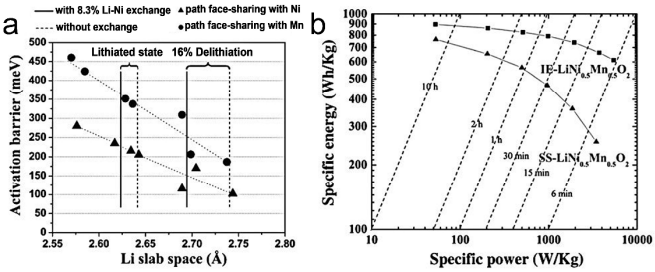

Figure 10. Typical examples for decreasing Li-ion diffusion energy: (a) Calculated activation barrier for Li^+ migration in $LiNi_{0.5}Mn_{0.5}O_2$ as a function of the Li slab space; (b) Ragone plot of the designed sample (IE) and controlled sample (SS) by traditional method.[35] Reproduced from Ref. 35 with permission from Science.

5. Electrode Architecture Engineering towards High-rate LIBs

Electrode structure engineering is a promising avenue to boost high-rate LIBs performance by maximizing ion and electron transport throughout the electrodes. The ideal electrode structure[45] should simultaneously provide: (i) an interconnected electrolyte-filled pore network that enables rapid ion transport, (ii) a short solid-phase ion diffusion length minimizing the effect of sluggish solid-state ion transport, (iii) a large electrode surface area, and (iv) high electron conductivity in the electrode assembly. Moreover, it should provide enough space for volume expansion preserving the structural integrity of the electrode during Li-ion insertion/extraction. Numerous efforts have been made to organize electrode materials into macroscale architectures. They can be structurally classified into 1D, 2D and 3D electrode structures (Figure 12), which allow the electron and ion to transport via one, two and three directions respectively. The recent works related to the multiple-dimensional electrode structures towards high-rate LIBs are summarized as follows.

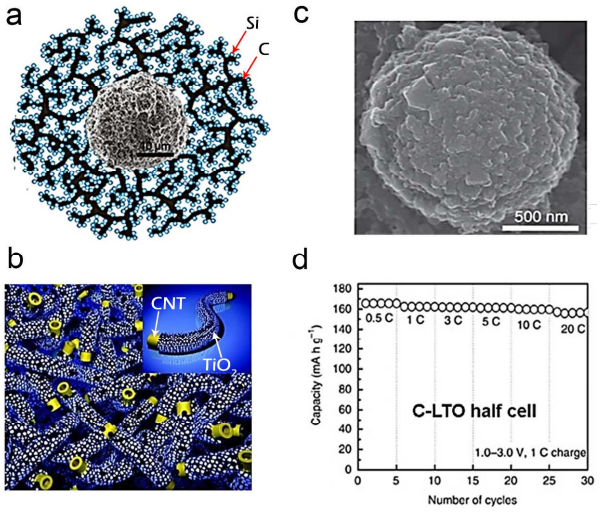

Figure 11. Hybrid-composite design: (a) Schematic and SEM image of Si-C nanocomposites granule;[40] (b) Schematic illustration of the effectively mixed conducting 3D networks of carbon nanotube CNT@TiO_2 core/porous-sheath coaxial nanocables.[41] (c) SEM images and (d) rate performance of the carbon-LTO particles.[43] Reproduced from Ref. 41 with permission from American Chemical Society. Reproduced from Ref. 40, 43 with permission from Nature Publishing Group.

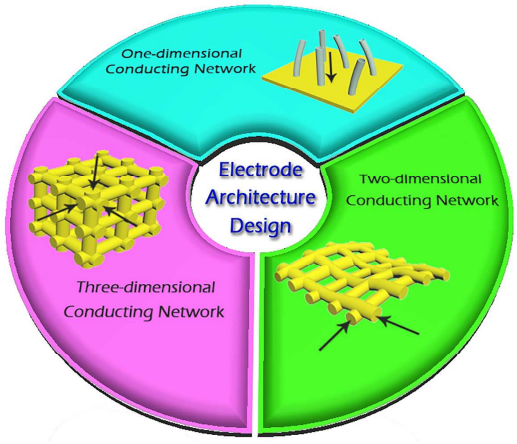

Figure 12. Electrode structure design strategies: one-dimensional, two-dimensional, three-dimensional conducting network electrode.

5.1 One-dimensional Conducting Network Electrode

A general structural strategy for high-rate LIBs electrodes is to grow 1D nanostructures (tube, wires, rods, etc.) directly on current collector without the usage of conductive additives or binders. This approach provides direct and short diffusion pathways for electron and ion, and the nanostructures can provide high contact surface area with the electrolytes. For examples, 1D Cu-Si-Al_2O_3 nanocable arrays electrode[46] (Figure 13a-b), in which the conductive Cu core-wire allowing for the effective electron transport to the substrate and the Al_2O_3 coating stabilizing the SEI layer, showed a high specific capacity of 790 mAh/g under high current density of 14 A/g while Cu-Si nanocables only show a small specific capacity of 48 mAh/g (Figure 13c). Likewise, vertically aligned LTO nanosheet arrays[47] (Figure 13d-e) exhibited an outstanding cycling performance with the capacity retention of 124 mAh/g after 3000 cycles at 50 C.

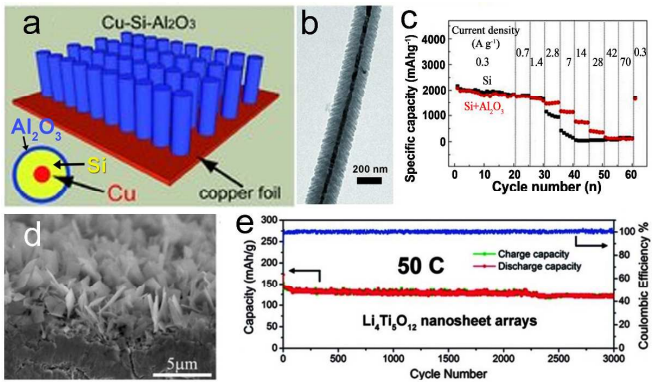

Figure 13. Direct growth of 1D nanostructures on conducting substrates: (a-b) Schematic diagram and TEM image of Cu-Si-Al_2O_3 nanocables respectively; (c) Comparison of the rate capabilities of Cu-Si-Al_2O_3 nanocables (red) and Cu-Si (black).[46] (d) SEM images of $Li_4Ti_5O_{12}$ nanosheet arrays standing on Ti foil; (e) Specific capacity and Coulombic efficiency of $Li_4Ti_5O_{12}$ nanosheet arrays.[47] Reproduced from Ref. 46 with permission from John Wiley & Sons Ltd. Reproduced from Ref. 47 with permission from Royal Society of Chemistry.

5.2 Two-dimensional Conducting Network Electrode

Besides the 1D charge transport to conducting substrate, 2D nanoarchitectures (e.g., metal meshes, carbon clothes) allow electron and ion to transport in two directions. In particular, the penetrable mesh structure is favorable for the ionic flow and exchange of electrolytes. Also, the porosity of the mesh can mitigate the effects of large volume expansion of electrode materials especially at high rate, extending their cycling life. For instance, a research work on a NiO/Ni mesh electrode (Figure 14a)[48] with a framework of the nickel mesh and mesoporous NiO film served as the electronic path and anode material respectively, showed a large capacity of 195 mAh/g at ultrahigh current density of 50 A/g (Figure 14b). Compared with the metal mesh, carbon materials such as carbon nanotubes, porous carbon, and graphene, are widely used for the conductive scaffold due to their excellent electrical conductivity, and electrochemical stability as well as the low cost. A hierarchical three-dimensional $ZnCo_2O_4$ nanowire arrays/carbon cloth composites[49] (Figure 14c-d) were synthesized for LIBs with the features of high reversible capacity and excellent cycling ability. It can be seen that the capacity decreases from 1200 to 605 mAh/g with increasing C-rate ranging from 0.2 to 5 C (Figure 14e). This concept using 2D conductive mesh or carbon cloth for high-rate

LIBs can be applied in flexible devices, and also can be extended to other devices like electrochemical capacitors and electronic devices.

5.3 Three-dimensional Conducting Network Electrode

Engineering 3D electrode structure offers great advantages for high-rate LIBs, such as enhancing ion and electron transport kinetic, increasing electrode/electrolyte contact area as well as improving mechanical stability during high-rate rechargeable cycling. In the following sections, the strategies to build up the 3D electrode structure with rational control of the ion and electron transport length, surface area, and electrode porosity towards high-rate performance of LIBs are discussed.

3D Bicontinuous Conducting Electrode Design: 3D conducting electrodes are built by using the continuous or quasi-continuous carbon- or metal- based porous framework on current collector. For instance, Paul V. Braun et al.[45] demonstrated a general paradigm to create ultrahigh-rate LIBs through the use of a 3D composite electrode based on nickel inverse opal (Figure 15a-b). Benefited from the bicontinuous conducting network, a LIBs prototype assembled from a lithiated MnO_2 cathode retains 76% of its capacity (at 1.1 C) when discharged at 185 C, and 38% when discharged at a huge rate of 1114 C (Figure 15c). Also, based on highly porous nickel scaffolds, 3D bicontinuous interdigitated microelectrodes based on the nickel–tin (anode) and lithiated manganese oxide (LMO) (cathode) were integrated to fabricate micro-LIBs (Figure 15d-e).[50] The battery microarchitecture, concurrently optimizing ion and electron transport for high-power delivery, realized a power density up to 7.4 mW/cm^2·μm, which equals or even exceeds that of the best supercapacitors, and is 2,000 times higher than that of other microbatteries. At high discharge rates of 1000 C, the cell retains a large percentage (ca. 28%) of its low-rate energy density at 0.5 C (Figure 15e).

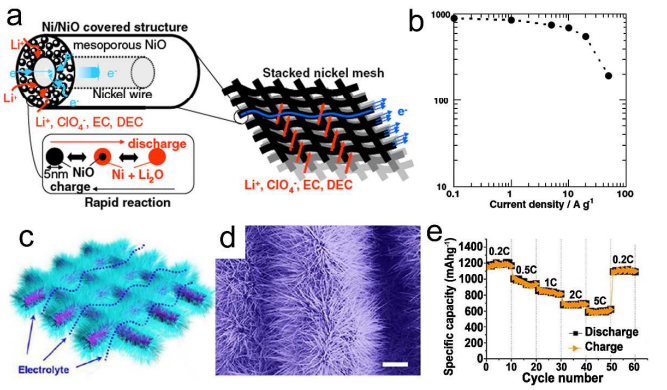

Figure 14. 2D conducting network based on (a-b) NiO/Ni mesh and (c-e) $ZnCo_2O_4$ nanowire arrays/carbon cloth anodes: (a) proposed electron and ion transport pathway and (b) the rate capability of NiO/Ni mesh.[48] (c) Schematic representation, (d) FESEM image, and (e) rate capability of $ZnCo_2O_4$ nanowire arrays/carbon cloth.[49] Reproduced from Ref. 48 with permission from Elsevier. Reproduced from Ref. 49 with permission from American Chemical Society.

Interestingly, an approach based on recently-emerged 3D printing technique, was used to fabricate 3D interdigitated microbattery architectures (3D-IMA) composed of LTO and $LiFePO_4$ (LFP).[51] The 3D-IMA demonstrated a high areal energy density of 9.7 J/cm^2 at a power density of 2.7 mW/cm^2. Beyond that, high-rate flexible LIBs were also developed due to their potential application in electronic systems such as roll-up displays and wearable devices. A lightweight and flexible LIBs made from graphene foam (GF) loaded with LTO and LFP,[52] delivered a capacity of 117 mAh/g at 10 C, which is 88% of the capacity at 1 C.

3D Long-range-networking Electrode Structure: Different from the building of bicontinuous conducting substrates or scaffolds with 3D hierarchical structures, the current concept is to develop a long-range conducting network electrode enabled by the 1D elongated nanostructured material itself with high aspect ratio, forming additive-free (free usage of binder and conductive agent or support) 3D mesoporous electrode architectures. For examples, Yang S. et al[53] reported a layer-by-layer (LBL) technique to assemble the functionalized conducting network of multiwalled carbon nanotubes (MWNTs) on current collector. The electrode with several micrometers thick, can store lithium ion up to a reversible capacity of ~200 mAh/g while also delivering a high power density of 100 kW/kg. Moreover, a device using MWNTs device using MWNTs and LTO had a power delivery ~10 times higher than that of conventional LIBs. Based on an electrospun-template method, Cui's group[17] realized the long double-walled Si-SiO_x nanotubes (DWSiNTs, Figure 16a), in which the inner wall is active silicon and the outer wall is the confining SiO_x. The battery exhibited charging capacities approximately eight times larger than conventional carbon anodes and charging rates of up to 20 C (Figure 16b). For the LBL method and electrospunning technology, the building of MWNTs and DWSiNTs 3D architectures with good adhesion to current collector is achieved by the electrostatic force and the polymerization of nanofiber network respectively. In our previous work, we developed a stirring hydrothermal method to prepare gel-like 1D TiO_2-based nanotubes with length up to tens of micrometers,[14] which adheres well on the current collector without usage of binder. The LIBs devices based on TiO_2(B) nanotubular cross-link network electrode exhibits superior cycling capacity (ca. 114 mAh/g) over 10000 cycles at high rate of 25 C (8.4 A/g) synchronized with ca. 100% Coulombic efficiency (Figure 16c).

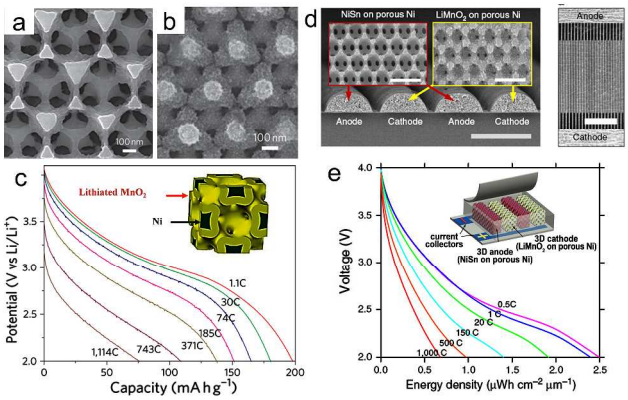

Figure 15. 3D Bicontinuous Conducting Electrode: SEM images of (a) nickel inverse opal and (b) lithiated MnO_2/nickel composite cathode; (c) Discharge behavior of the ultrafast LIBs based on bicontinuous lithiated MnO_2 cathode (Inset is the bicontinuous electrode model).[45] (d) Cross-section and top-down SEM images of the interdigitated microelectrodes.[50] (e) Discharge curve of microbattery cell at various C rates; the inset is the microbattery design schematic. Reproduced from Ref. 45 and 50 with permission from Nature Publishing Group.

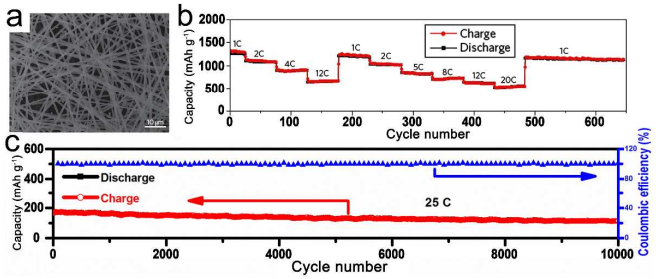

Figure 16. Long-range-networking electrode materials for high-rate LIBs: (a) SEM images and (b) rate performance of DWSiNTs.[17] (c) Long-term cycling performance of TiO_2(B) nanotubes at 25 C.[14] Reproduced from Ref. 14 with permission from John Wiley & Sons Ltd. Reproduced from Ref. 17 with permission from Nature Publishing Group.

6. Conclusions and Outlook

Ultrafast rechargeable LIBs with high charging rate (> 10 C) are highly demanded in portable electronics and electrical vehicles nowadays. That is, the energy storage device should possess the supercapacitor-like rate performance and battery-like capacity as well as long-expectancy. However, the rate capability of state-of-art commercialized LIBs system is difficult to meet the increasing market demands, especially for the electrical vehicles. In this tutorial review, we have reviewed the key developments on the rational design of advanced electrode materials and their corresponding electrode architectures for achieving ultrafast rechargeable LIBs. Through the understanding of the basic electrochemistry and the viewpoints of conduction mechanism for Li-ion and electron in four transport steps (Figure 2), it is advised that maximizing both ion and electron transport in solid-state diffusion of the electrode materials is of critical importance. From materials chemistry perspectives, the promising anode and cathode materials should possess high intrinsic electronic conductivity and lithium ion diffusivity, high electrochemical reaction kinetics, short diffusion length and robust nanostructure under the rapid insert/removal of Li-ion from the electrode materials.

However, the current-state developed electrode materials do not have the above ideal properties. Therefore, the rational materials design is required to compensate their intrinsic weak functionality. From the materials engineering aspect, promising approaches and new concepts are adopted to achieve high-rate performance of LIBs. As described above, key strategies, including development of the nano-size materials with high surface areas, doping technology, surface modification, and lithium ion diffusion control, can contribute to enhancements of electron and ion diffusion rates inside or surface of the active materials significantly. On the other aspect, electrode architecture design, is also particularly powerful for facilitating ionic and electronic transport even for electrode materials with low intrinsic conductivity. These methods include the design of 1D, 2D and 3D electrode architectures, which allow the electron and ion to transport via multiple directions to the current collector. In particular, the 3D electrode architecture strategies like bicontinuous conducting electrode design and long-range-networking electrode structure can improve the LIBs rate performance greatly owing to shorter diffusion length, more reactive area from mesoporous structure as well as improved structure stability.

Despite that the rational materials design for high-rate LIBs have been well documented, continuous efforts are necessary to develop advanced functional electrode materials or structure towards the commercialization of ultrahigh-rate LIBs. To this aim, important aspects need to be considered to shape the future of ultrafast charging LIBs. Firstly, the combined theoretical and experimental study will assist us to develop the promising new electrode materials in terms of the rate capability and long-cycling ability. The material candidates with higher capacity and larger potential difference between the anode and cathode materials are preferred for boosting both high energy- and power- density. Moreover, since the batteries are complex systems, it is also important to develop multiscale modeling tools for fundamental understanding, diagnostics and design of new electrochemical materials and their operation conditions to optimize overall cell performance, which can be referred from the recent review paper.[54] Secondly, high-rate LIBs require both the anode and cathode materials possess high-rate capability simultaneously. However, current material designs for high-rate LIBs mainly focus on half-cell system. Toward the practical full cell battery for high-rate application, the maximum matching of the cathode and anode materials in terms of rate capability and the capacity is required, and the optimization of their electrode structure for ideal ionic and electronic transport is also crucial. Thirdly, SEI layer protects the electrode from chemically reacting with the electrolyte. However, SEI layer also affects the behavior of ion diffusion and electron transfer at the electrode materials surface and thus plays an important role on rate capabilities. Thus, the systematic study of the SEI layer with electrochemically stable, high ionic conductivity, as well as low resistance is needed. Fourthly, from the viewpoint of sustainability and ecoefficiency, organic materials may evolve the energy storage device in terms of ultrafast charging,[43] long-time stability, as well as high capacity although currently most of the electrode materials are based on inorganic materials. Finally, the risk of ultrafast charging LIBs and safety management remain an important yet under-researched field. In particular, the potential safety issue due to fast generation of heat needs be considered when the batteries are charged/discharged at high current density. One of the important aspects is to develop the safe electrolyte systems with high ionic conductivity and non-flammable property (Section 2.4). For example, a new developed lithium superionic conductor showed a very high ionic conductivity (1.2×10^{-2} S/cm),[8] which is a promising solid electrolyte for fast ionic transport.

Currently, the ultrafast charging technology is gaining global attentions and several companies have launched their products, like Toshiba SCiB (lithium titanate) and A123 systems (lithium iron phosphate) batteries, allowing the battery to be charged within 10 min. Besides that, more and more rapid-charging prototypes are under development to meet the PEV goal (Figure 2). Based on the fundamental understanding on the working principles of LIBs and design guidance for rational material-design towards high-rate LIBs, continuing efforts and breakthrough concepts are urgently required to overcome the current challenges of ultrahigh-rate LIBs to achieve high power and energy density, and their practical applications will herald a new paradigm for energy storage systems, accelerating the commercialization of battery electrical vehicles in the near future.

Acknowledgements

This work was supported by the National Research Foundation (NRF), Prime Minister's Office, Singapore under its Campus for Research Excellence and Technological Enterprise (CREATE) Programme of Nanomaterials for Energy and Water management.

References

1. P. Simon, Y. Gogotsi and B. Dunn, *Science*, 2014, **343**, 1210-1211.
2. P. V. Braun, J. Cho, J. H. Pikul, W. P. King and H. Zhang, *Curr. Opin. Solid State Mater. Sci.*, 2012, **16**, 186-198.

3. J. B. Goodenough and K. S. Park, *J. Am. Chem. Soc.*, 2013, **135**, 1167-1176.
4. M. Winter and R. J. Brodd, *Chem. Rev.*, 2004, **104**, 4245-4269.
5. H. Mehrer, *Diffusion in Solids: Fundamentals, Methods, Materials, Diffusion-Controlled Processes*, Springer, New York, 2007.
6. M. Park, X. Zhang, M. Chung, G. B. Less and A. M. Sastry, *J. Power Sources*, 2010, **195**, 7904-7929.
7. M. A. Quiroga, K.-H. Xue, N. Trong-Khoa, M. Tulodziecki, H. Huang and A. A. Franco, *J. Electrochem. Soc.*, 2014, **161**, E3302-E3310.
8. N. Kamaya, K. Homma, Y. Yamakawa, M. Hirayama, R. Kanno, M. Yonemura, T. Kamiyama, Y. Kato, S. Hama, K. Kawamoto and A. Mitsui, *Nature Mater.*, 2011, **10**, 682-686.
9. M. R. Palacin, *Chem. Soc. Rev.*, 2009, **38**, 2565-2575.
10. R. E. Hummel, *Electronic Properties of Materials*, Springer, New York, 2011.
11. C. M. Hayner, X. Zhao and H. H. Kung, *Annu. Rev. Chem. Biomol. Eng.*, 2012, **3**, 445-471.
12. G.-N. Zhu, H.-J. Liu, J.-H. Zhuang, C.-X. Wang, Y.-G. Wang and Y.-Y. Xia, *Energy Environ. Sci.*, 2011, **4**, 4016-4022.
13. A. G. Dylla, G. Henkelman and K. J. Stevenson, *Acc. Chem. Res.*, 2013, **46**, 1104-1112.
14. Y. Tang, Y. Zhang, J. Deng, J. Wei, H. L. Tam, B. K. Chandran, Z. Dong, Z. Chen and X. Chen, *Adv. Mater.*, 2014, **26**, 6111-6118.
15. V. Augustyn, J. Come, M. A. Lowe, J. W. Kim, P.-L. Taberna, S. H. Tolbert, H. D. Abruña, P. Simon and B. Dunn, *Nature Mater.*, 2013, **12**, 518-522.
16. M. M. Thackeray, C. Wolverton and E. D. Isaacs, *Energy Environ. Sci.*, 2012, **5**, 7854-7863.
17. H. Wu, G. Chan, J. W. Choi, I. Ryu, Y. Yao, M. T. McDowell, S. W. Lee, A. Jackson, Y. Yang, L. B. Hu and Y. Cui, *Nature Nanotech.*, 2012, **7**, 309-314.
18. P. Poizot, S. Laruelle, S. Grugeon, L. Dupont and J. M. Tarascon, *Nature*, 2000, **407**, 496-499.
19. J. Wang, N. Yang, H. Tang, Z. Dong, Q. Jin, M. Yang, D. Kisailus, H. Zhao, Z. Tang and D. Wang, *Angew. Chem. Int. Ed.*, 2013, **52**, 6417-6420.
20. M. S. Islam and C. A. J. Fisher, *Chem. Soc. Rev.*, 2014, **43**, 185-204.
21. B. Xu, D. Qian, Z. Wang and Y. S. Meng, *Mat. Sci. Eng. R.*, 2012, **73**, 51-65.
22. J. Lee, A. Urban, X. Li, D. Su, G. Hautier and G. Ceder, *Science*, 2014, **343**, 519-522.
23. J. M. Feckl, K. Fominykh, M. Döblinger, D. Fattakhova-Rohlfing and T. Bein, *Angew. Chem. Int. Ed.*, 2012, **51**, 7459-7463.
24. H. Wang, T. A. Tan, P. Yang, M. O. Lai and L. Lu, *J. Phy. Chem. C*, 2011, **115**, 6102-6110.
25. Y. Tang, Y. Zhang, J. Deng, D. Qi, W. R. Leow, J. Wei, S. Yin, Z. Dong, R. Yazami, Z. Chen and X. Chen, *Angew. Chem. Int. Ed.*, 2014, **53**, 13488-13492.
26. S. Lee, Y. Cho, H. K. Song, K. T. Lee and J. Cho, *Angew. Chem. Int. Ed.*, 2012, **51**, 8748-8752.
27. K. T. Nam, D.-W. Kim, P. J. Yoo, C.-Y. Chiang, N. Meethong, P. T. Hammond, Y.-M. Chiang and A. M. Belcher, *Science*, 2006, **312**, 885-888.
28. K.-S. Park, A. Benayad, D.-J. Kang and S.-G. Doo, *J. Am. Chem. Soc.*, 2008, **130**, 14930-14931.
29. Y.-Q. Wang, L. Gu, Y.-G. Guo, H. Li, X.-Q. He, S. Tsukimoto, Y. Ikuhara and L.-J. Wan, *J. Am. Chem. Soc.*, 2012, **134**, 7874-7879.
30. B. Kang and G. Ceder, *Nature*, 2009, **458**, 190-193.
31. Y.-K. Sun, Z. Chen, H.-J. Noh, D.-J. Lee, H.-G. Jung, Y. Ren, S. Wang, C. S. Yoon, S.-T. Myung and K. Amine, *Nature Mater.*, 2012, **11**, 942-947.
32. Z.-S. Wu, W. Ren, L. Xu, F. Li and H.-M. Cheng, *ACS Nano*, 2011, **5**, 5463-5471.
33. L. Shen, E. Uchaker, X. Zhang and G. Cao, *Adv. Mater.*, 2012, **24**, 6502-6506.
34. S.-T. Myung, M. Kikuchi, C. S. Yoon, H. Yashiro, S.-J. Kim, Y.-K. Sun and B. Scrosati, *Energy Environ. Sci.*, 2013, **6**, 2609-2614.
35. K. Kang, Y. S. Meng, J. Bréger, C. P. Grey and G. Ceder, *Science*, 2006, **311**, 977-980.
36. C. Delmas, M. Maccario, L. Croguennec, F. Le Cras and F. Weill, *Nature Mater.*, 2008, **7**, 665-671.
37. L. Wang, X. He, W. Sun, J. Wang, Y. Li and S. Fan, *Nano Lett.*, 2012, **12**, 5632-5636.
38. X. Rui, X. Zhao, Z. Lu, H. Tan, D. Sim, H. H. Hng, R. Yazami, T. M. Lim and Q. Yan, *ACS Nano*, 2013, **7**, 5637-5646.
39. A. Mukhopadhyay, F. Guo, A. Tokranov, X. Xiao, R. H. Hurt and B. W. Sheldon, *Adv. Funct. Mater.*, 2013, **23**, 2397-2404.
40. A. Magasinski, P. Dixon, B. Hertzberg, A. Kvit, J. Ayala and G. Yushin, *Nature Mater.*, 2010, **9**, 353-358.
41. F.-F. Cao, Y.-G. Guo, S.-F. Zheng, X.-L. Wu, L.-Y. Jiang, R.-R. Bi, L.-J. Wan and J. Maier, *Chem. Mater.*, 2010, **22**, 1908-1914.
42. L. Li, A.-R. O. Raji and J. M. Tour, *Adv. Mater.*, 2013, **25**, 6298-6302.
43. H.-G. Jung, M. W. Jang, J. Hassoun, Y.-K. Sun and B. Scrosati, *Nature Commun.*, 2011, **2**, 516.
44. W. Guo, Y.-X. Yin, S. Xin, Y.-G. Guo and L.-J. Wan, *Energy Environ. Sci.*, 2012, **5**, 5221-5225.
45. H. Zhang, X. Yu and P. V. Braun, *Nature Nanotech.*, 2011, **6**, 277-281.
46. F.-F. Cao, J.-W. Deng, S. Xin, H.-X. Ji, O. G. Schmidt, L.-J. Wan and Y.-G. Guo, *Adv. Mater.*, 2011, **23**, 4415-4420.
47. S. Chen, Y. Xin, Y. Zhou, Y. Ma, H. Zhou and L. Qi, *Energy Environ. Sci.*, 2014, **7**, 1924-1930.
48. E. Hosono, S. Fujihara, I. Honma and H. Zhou, *Electrochem. Commun.*, 2006, **8**, 284-288.
49. B. Liu, J. Zhang, X. Wang, G. Chen, D. Chen, C. Zhou and G. Shen, *Nano Lett.*, 2012, **12**, 3005-3011.
50. J. H. Pikul, H. Gang Zhang, J. Cho, P. V. Braun and W. P. King, *Nat. Commun.*, 2013, **4**, 1732.
51. K. Sun, T.-S. Wei, B. Y. Ahn, J. Y. Seo, S. J. Dillon and J. A. Lewis, *Adv.Mater.*, 2013, **25**, 4539-4543.
52. N. Li, Z. Chen, W. Ren, F. Li and H.-M. Cheng, *Proc. Natl Acad. Sci. USA*, 2012, **109**, 17360-17365.
53. S. W. Lee, N. Yabuuchi, B. M. Gallant, S. Chen, B.-S. Kim, P. T. Hammond and Y. Shao-Horn, *Nature Nanotech.*, 2010, **5**, 531-537.
54. A. A. Franco, *RSC Adv.*, 2013, **3**, 13027-13058.